Chapter 4

Origin of Charge Transfer Exciton Dissociation in Organic Solar Cells

Shota Ono and Kaoru Ohno

Additional information is available at the end of the chapter

http://dx.doi.org/10.5772/intechopen.69854

Abstract

Using a temperature (T)-dependent tight-binding (TB) model for an electron-hole pair at the donor-acceptor (DA) interface, we investigate the dissociation of charge transfer exciton (CTE) into free carriers, that is, an electron and a hole. We observe the existence of the localization-delocalization transition at a critical T, below which the charges are localized to the DA interface, and above which the charges are delocalized over the system. This explains the CTE dissociation observed in organic solar cells. The present study highlights the combined effect of finite T and carrier delocalization in the CTE dissociation.

Keywords: charge transfer exciton, localization-delocalization transition, donor-accepter interface, tight-binding model, temperature

1. Introduction

Exciton, which is a two-particle state of electron and hole created by photon absorption of semiconductors or insulators, has been extensively studied since the seminal works of Frenkel [1, 2] and Wannier [3]. The binding energy of the exciton determines the photon absorption spectra near the band edges, where the Rydberg series, similar to the hydrogen-like excitation spectra, can be observed [4]. The concept of excitons is valid not only in solids but also in complex systems, such as nanostructures and interfaces. For example, let us consider two molecules with an appropriate separation. Given an electron-hole (EH) pair created in one molecule by a photon absorption, an electron in the molecule would be transferred to the other molecule due to the different lowest unoccupied molecular orbital (LUMO) energies, while a hole is left behind. Since the electron in the latter molecule and the hole in the former molecule interact with each other via the Coulomb interaction forces, they form a bound state, called as the charge transfer exciton (CTE) [5]. Recently, the CTE near the organic semiconductor interfaces has attracted much interest in the field of organic solar cells [6, 7]. This is a main concern in this chapter.

Organic solar cells, which generate electric power from the sunlight, play an important role in green energy industry and possess a variety of advantages: low cost, light, flexibility and easy-fabrication. The organic solar cells consist of the heterojunction between the electron donor and electron acceptor molecules. For example, in the C_{60}-based solar cells, the C_{60}-molecules serve as the accepter molecule and the organic thin-films such as X-phthalocyanine (XPc, X = Cu, Zn) [8–12] and single-walled carbon nanotubes [13, 14] serve as the donor molecules.

The principle of power generation in organic solar cells is decomposed into three steps, as shown in **Figure 1**: (i) exciton creation at the donor site by photon absorption, (ii) CTE creation following the movement of the created excitons to the donor-accepter (DA) interface and (iii) charge generation by the CTE dissociation into free carriers. While the second step may occur due to the different LUMO energies between the donor and acceptor molecules, the microscopic mechanism of the third step has not been understood; Since the CTE binding energy is a few hundreds of meV [6, 7, 15], the thermal energy is not enough to separate the EH pair into free carriers. In this way, several effects, such as dark dipoles [16, 17], disorder [18, 19], carrier delocalization [20–23], light effective mass [24] and entropy [25–28], on the CTE dissociation have been investigated. However, the relative importance of these factors is under debate.

In this chapter, we present an origin of the CTE dissociation by investigating the EH pair at the DA interface within a temperature (T)-dependent tight-binding (TB) model [29]. The important fact is that there exists a localization-delocalization transition at a critical T. The transition temperature estimated is in agreement with experimental observations in semiconductor interfaces [27]. Based on the T-dependence of the EH pair energy, we interpret the EH pair dynamics observed in time-resolved two-photon photoemission experiments [28]. Our model has shown that the transition can be observed only when the finite-T and the carrier delocalization effects are simultaneously considered. This review provides an important fact that more than one phenomenon might contribute to CTE dissociation.

The reminder of this chapter is organized as follows. In Section 2, we review the previous models of the CTE dissociation in organic solar cells. How the carrier delocalization effect is important in understanding the CTE dissociation is discussed. In Section 3, we present the formulation of the T-dependent TB model and the numerical results on the CTE dissociation. Our model is distinct from others in that the finite-T as well as the carrier delocalization effect is taken into account. In Section 4, how our model interprets the experimental data is discussed. Summary is presented in Section 5.

2. Literature review

We shall describe briefly some of the works that have theoretically discussed the origin of the CTE dissociation at the DA interface. The models can be classified into three levels on the basis of the approximation made (I) both charges, that is, electron and hole, are treated as localized particles [**Figure 2(a)**]; (II) one of the charges is treated as a delocalized particle, while the other is still treated as a localized one [**Figure 2(b)**] and (III) both charges are treated as delocalized

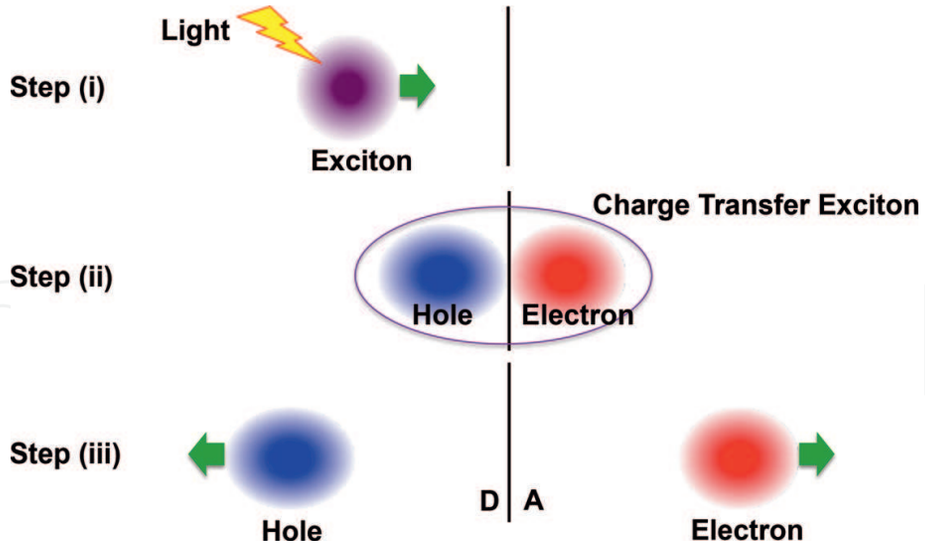

Figure 1. Schematic illustration of power generation in organic solar cells. The CTE, enclosed by an ellipse, consists of the electron and hole at the acceptor and donor, respectively. The donor and acceptor regions are abbreviated by D and A, respectively.

particles [**Figure 2(c)**], where the motion of the localized and delocalized particles would be described within the classical (or semi-classical) and quantum mechanics, respectively.

In the earliest study, Arkhipov et al. have constructed a dark dipole model within the approximation (I) above [16]. In this model, the DA interface consists of several polymer chains parallel to the DA interface. They computed the total energy of the CTE, that is, the sum of the electrostatic potential energy and the kinetic energy of the zero-point oscillations, by assuming the presence of the several dipoles at the DA interface. While the movement of the charged particle away from the interface lowers the Coulomb attractive forces, it also decreases the kinetic energy. They have found that the latter overcomes the former when the effective mass of the charged particle is less than $0.3m_e$, where m_e is the free electron mass, yielding the CTE dissociation. The effect of the different numbers of dipoles at the DA interface has also been investigated [17].

Deibel et al. have pointed out the importance of the charge delocalization along the polymer chains on the CTE dissociation by performing the kinetic Monte Carlo simulations [20]. To rationalize the concept of the delocalization, Nenashev et al. have developed an analytical model for the CTE dissociation within the approximation (II) [21]. They also studied the dissociation rate as a function of applied electric field by using the Miller-Abrahams expression for the hopping rate [30] and the dissociation probability formula for one-dimensional lattices [19]. The model has been further improved to include the effect of the dark dipoles at the DA interface [24]. However, those models have still employed the crude approximation (II) that one of the particles is fixed at a site.

Within the treatment (III), Raos et al. have computed the distribution of the electron and hole near the DA interface [22]. Using the TB approximation, they have shown that the sites where charge concentrates are not necessarily those just next to the DA interface, and this holds even

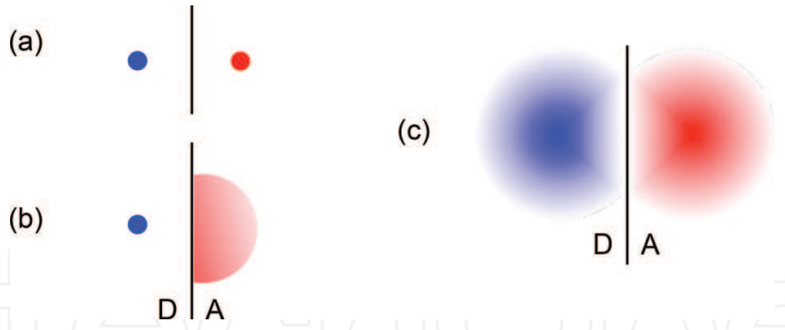

Figure 2. Schematic illustration of charged particles at the DA interface. (a) Localized hole and localized electron, (b) Localized hole and delocalized electron, and (c) delocalized hole and delocalized electron. Figures extracted and edited from Ref. [29].

in the ground state if diagonal and/or off-diagonal disorder exists. Athanasopoulos et al. have also confirmed that the CTE can efficiently dissociate into free carriers by extending the Arkhipov-Nenashev model above [23]. Recently, the authors have developed a *T*-dependent TB model applicable to the EH pair motion at the DA interface [29]. It has been shown that there exists a localization-delocalization transition of the EH pair at a critical *T*, below which the charges are localized to the DA interface, and above which the charges are delocalized over the system. This will be demonstrated below.

3. Localization-delocalization transition of EH pair

3.1. Formulation

We briefly provide the *T*-dependent TB model for describing the EH pair distribution at the DA interface. The details of the model have been provided in Ref. [29]. A similar approach has been used to study the size-dependent exciton energy of the quantum dots at zero *T* [31]. First, we consider an EH pair near the DA interface, assuming that only one photon is absorbed and that the electron-electron and hole-hole interaction energies are negligible. The electron and hole move around the acceptor and donor region, respectively, while they interact with each other via the attractive Coulomb interaction forces. Then, the Schrödinger equation for the two particles is given by

$$H^{(i)}|\phi_\alpha^{(i)}\rangle = \varepsilon_\alpha{}^{(i)}|\phi_\alpha^{(i)}\rangle, \tag{1}$$

where $\phi_\alpha^{(i)}$ and $\varepsilon_\alpha^{(i)}$ are the eigenfunction and eigenenergy with a quantum number α for the electron (i = e) and hole (i = h). Using the TB approximation, the Hamiltonian is given by

$$H^{(i)} = -\Sigma_{p,p'} t_{p,p'}^{(i)} |\boldsymbol{p}\rangle\langle\boldsymbol{p}'| + \Sigma_p V_p^{(i)} |\boldsymbol{p}\rangle\langle\boldsymbol{p}|, \tag{2}$$

where the first and second term denotes the kinetic and potential energies for the particle i, respectively. $t_{p,p'}^{(i)}$ and $V_p^{(i)}$ are the hopping integral between sites $\boldsymbol{p}$ and $\boldsymbol{p}'$ and the on-site potential energy at the site $\boldsymbol{p} = (p_x, p_y, p_z)$ with integers p_x, p_y, and p_z. The former is set to

$t^{(i)}_{\boldsymbol{p},\boldsymbol{p}'} = t_0$, where t_0 is a positive constant, for simplicity. The effect of the long-range and anisotropic hopping has been investigated in Ref. [29]. The latter is explicitly given as

$$V^{(e)}_{\boldsymbol{p}} = w^{(e)}_{\boldsymbol{p}} - U_0 \Sigma_{\boldsymbol{p}'} \frac{1}{|\boldsymbol{p} - \boldsymbol{p}'|} n^{(h)}_{\boldsymbol{p}'}, \tag{3}$$

$$V^{(h)}_{\boldsymbol{p}} = w^{(h)}_{\boldsymbol{p}} - U_0 \Sigma_{\boldsymbol{p}'} \frac{1}{|\boldsymbol{p} - \boldsymbol{p}'|} n^{(e)}_{\boldsymbol{p}'}, \tag{4}$$

where U_0 determines the strength of the Coulomb interaction energy between the electron and hole. $w^{(i)}_{\boldsymbol{p}}$ is the potential barrier height for the particle i, which will be given below. $n^{(i)}_{\boldsymbol{p}}$ is the charge density for the particle i and is defined as

$$n^{(i)}_{\boldsymbol{p}} = \Sigma^{all}_{\alpha} f^{(i)}_{\alpha} |\langle \boldsymbol{p} | \phi^{(i)}_{\alpha} \rangle|^2, \tag{5}$$

where $|\langle \boldsymbol{p} | \phi^{(i)}_{\alpha} \rangle|^2$ is the probability amplitude of the site $\boldsymbol{p}$ for the eigenstate $\phi^{(i)}_{\alpha}$. The summation is taken over the all eigenstates weighted by the Fermi distribution function $f^{(i)}_{\alpha}$ defined as

$$f^{(i)}_{\alpha} = \{\exp[\beta(\varepsilon_{\alpha}{}^{(i)} - \mu^{(i)})] + 1\}^{-1} \tag{6}$$

with the inverse temperature (β) and the chemical potential $\mu^{(i)}$, which will be determined by the relation of

$$\Sigma_{\boldsymbol{p}} n^{(e)}_{\boldsymbol{p}} = \Sigma_{\boldsymbol{p}} n^{(h)}_{\boldsymbol{p}} = 1. \tag{7}$$

The self-consistent solution of Eqs. (1)–(7) yields the electron and hole distributions near the DA interface. The solution enables us to compute the T-dependence of the free energy

$$\Omega = U_{\text{int}} - TS \tag{8}$$

with the internal energy

$$U_{\text{int}} = \Sigma_{i=e,h} \Sigma_{\alpha} \varepsilon_{\alpha}{}^{(i)} f^{(i)}_{\alpha} + U_0 \Sigma_{\boldsymbol{p}} \Sigma_{\boldsymbol{p}'} \frac{1}{|\boldsymbol{p} - \boldsymbol{p}'|} n^{(e)}_{\boldsymbol{p}} n^{(h)}_{\boldsymbol{p}'} \tag{9}$$

and the entropic energy

$$-TS = k_B T \Sigma_{i=e,h} \Sigma_{\alpha} \left[f^{(i)}_{\alpha} \ln f^{(i)}_{\alpha} + (1 - f^{(i)}_{\alpha}) \ln(1 - f^{(i)}_{\alpha}) \right], \tag{10}$$

where S denotes the entropy and k_B is the Boltzmann constant. Below, the hopping parameter t_0 will be used as an energy unit.

For later use, we define the charge density integrated over the p_x - p_y plane parallel to the interface

$$Q^{(i)}_{\text{tot}}(p_z) = \Sigma_{p_x} \Sigma_{p_y} n^{(i)}_{\boldsymbol{p}} \tag{11}$$

with $i = e$ and h.

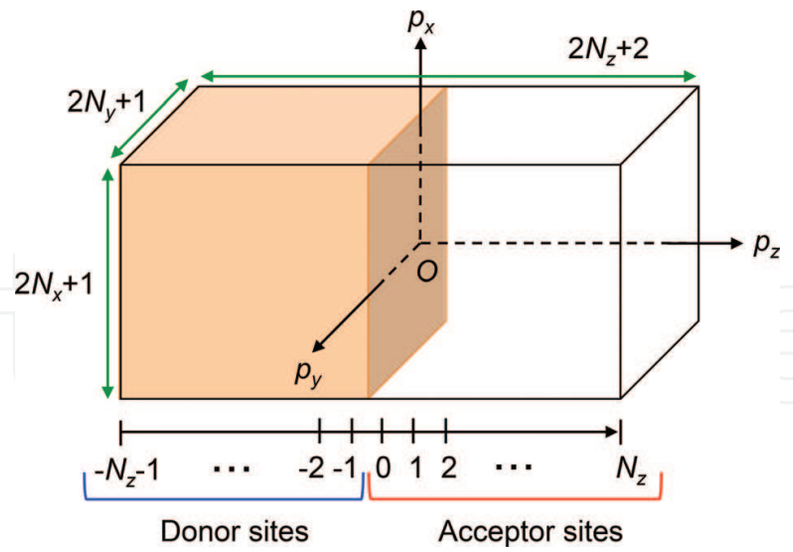

Figure 3. Simple cubic lattice for the DA interface model. The donor and acceptor regions are $-N_z - 1 \le p_z \le -1$ and $0 \le p_z \le N_z$, respectively. The total number of sites is $(2N_x + 1)(2N_y + 1)(2N_z + 2)$. Figure extracted from Ref. [29].

Figure 3 shows the DA interface model, where the simple cubic lattice is assumed. The movement of the electron and hole is restricted to the region of $-N_x \le p_x \le N_x$, $-N_y \le p_y \le N_y$, and $-N_z - 1 \le p_z \le N_z$. The potential barrier is assumed to be

$$w_{\boldsymbol{p}}^{(e)} = w_0 \theta(-0.5 - p_z), \tag{12}$$

$$w_{\boldsymbol{p}}^{(h)} = w_0 \theta(0.5 + p_z), \tag{13}$$

where $\theta(x)$ is the Heaviside step function, where $\theta(x) = 1$ for $x > 0$ and $\theta(x) = 0$ for $x < 0$. The numerical parameters in the model are set to $(N_x, N_y, N_z) = (5, 5, 10)$, $w_0 = 10t_0$, and $U_0 = 10t_0$, yielding the electron and hole that localize only to the acceptor and donor region, respectively at $T = 0$.

3.2. Numerical Results

Figure 4(a) shows the p_z-dependence of $Q_{\mathrm{tot}}^{(e)}(p_z)$ and $Q_{\mathrm{tot}}^{(h)}(p_z)$ in Eq. (11) for $k_B T/t_0 = 0$, 0.3, and 0.5. At zero T, $Q_{\mathrm{tot}}^{(e)}(p_z)$ ($Q_{\mathrm{tot}}^{(h)}(p_z)$) has the maximum value of 0.8 at $p_z = 0$ ($p_z = -1$) and decays within a few positive (negative) p_zs. As T increases, the p_z-dependence of $Q_{\mathrm{tot}}^{(e)}(p_z)$ and $Q_{\mathrm{tot}}^{(h)}(p_z)$ changes dramatically at around $k_B T/t_0 \simeq 0.3$: The values of $Q_{\mathrm{tot}}^{(e)}(p_z)$ and $Q_{\mathrm{tot}}^{(h)}(p_z)$ have the maximum of 0.3 at the sites away from those just next to the interface, that is, $p_z = 1$ and $p_z = -2$, respectively, and are averaged out over all p_z, which clearly indicate the CTE dissociation.

The localization-delocalization transition observed in **Figure 4(a)** can be understood as the free-energy anomaly. **Figure 4(b)** shows Ω in Eq. (8) as a function of T. The anomaly in Ω is observed at a critical temperature $k_B T_c/t_0 \simeq 0.27$. Ω is almost independent of T below T_c, while Ω decreases monotonically with increasing T above T_c. **Figure 4(c)** shows the T-dependence of the internal energy U_{int} and the entropy $-TS$ defined as Eqs. (9) and (10), respectively. Similar

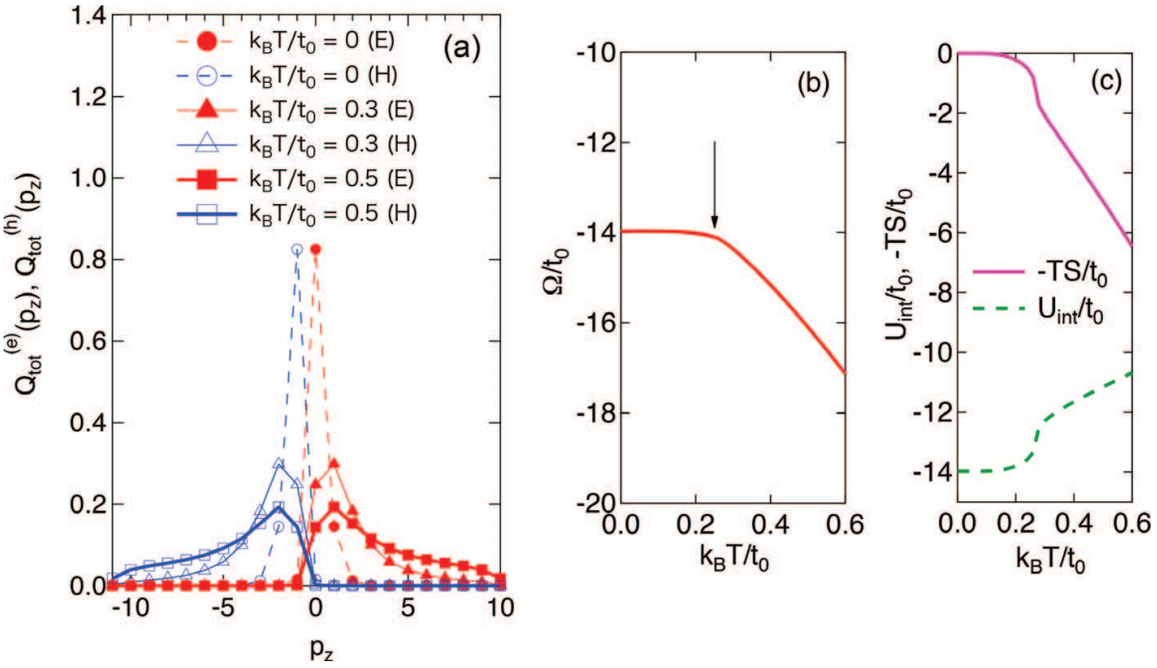

Figure 4. (a) The p_z dependence of $Q_{tot}^{(e)}$ (filled) and $Q_{tot}^{(h)}$ (open) given by Eq. (11) for $k_BT/t_0 = 0$ (circle), 0.3 (triangle), and 0.5 (square). The values of U_0/t_0 and w_0/t_0 are set to 10. (b) The T dependence of the free energy $\Omega(T)$ given by Eq. (8). The arrow indicates the free-energy anomaly that originates from the localization-delocalization transition. (c) U_{int} in Eq. (9) and $-TS$ in Eq. (10) as a function of T. Figures extracted and edited from Ref. [29].

anomalies are also observed in the T-dependence of U_{int} and $-TS$; U_{int} and $-TS$ jump at $T = T_c$, below which U_{int} and $-TS$ are almost independent of T, and above which U_{int} and $-TS$ increases and decreases, respectively. Since $S \simeq 0$ below T_c, Ω is dominated by the contribution from U_{int}. On the other hand, Ω is dominated by the entropy contribution above T_c.

To understand the microscopic mechanism of the localization-delocalization transition, we compute the density-of-states (DOS) for the EH pair, where the EH pair energy is defined as $E_\alpha^{(eh)} = \varepsilon_\alpha^{(e)} + \varepsilon_\alpha^{(h)}$. **Figure 5(a)** and **(b)** show the EH DOS at $k_BT/t_0 = 0$ and 0.6, respectively. At lower T, we can observe several peaks below the band edge: $E_\alpha^{(eh)} = -19.9, \ -17.1$ (doubly degenerate), and 16.4 eV. On the other hand, at higher T, no peaks are observed. **Figure 6(a)** shows the charge density of the electron and hole for the lowest 10 energy peaks at $T = 0$. The charge density is localized to the DA interface at lower $E_\alpha^{(eh)}$, while it is delocalized over the system at higher $E_\alpha^{(eh)}$. Note that at the lowest T the occupation probability of the lowest energy state is unity. When T is increased, the eigenvalue distribution changes. This is because the Fermi distribution function in Eq. (6) is broadened. This leads to the decrease in the Coulomb attractive forces between the electron and hole, yielding an upper shift of the EH pair energy. **Figure 6(b)** shows the T-dependence of $E_\alpha^{(eh)}$ for $\alpha = 1-10$. In fact, $E_\alpha^{(eh)}$ increases as T increases. The important fact is that the value of $E_\alpha^{(eh)}$ drastically increases at $T = 0.3t_0$, above which the energy level spacing is small compared to that below T_c. This yields the absence of peaks in the DOS near the band edge, shown in **Figure 5(b)**. The absence of isolated peaks means that all eigenstates are delocalized, indicating the localization-delocalization transition at a critical T.

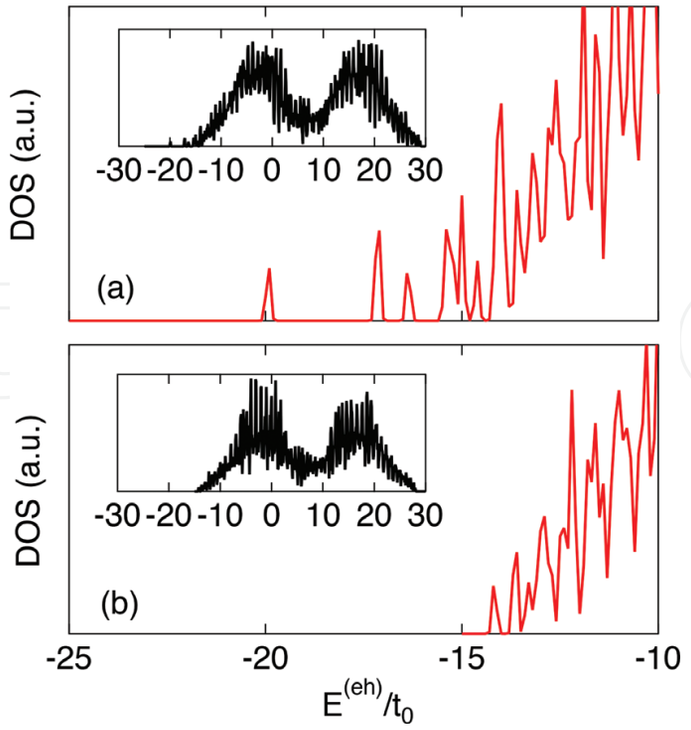

Figure 5. Electron-hole DOS (a) for $k_BT/t_0 = 0$ and (b) $k_BT/t_0 = 0.6$ from $E^{(eh)}/t_0 = -25$ to -10. The whole DOS is shown in the inset. Figures extracted from Ref. [29].

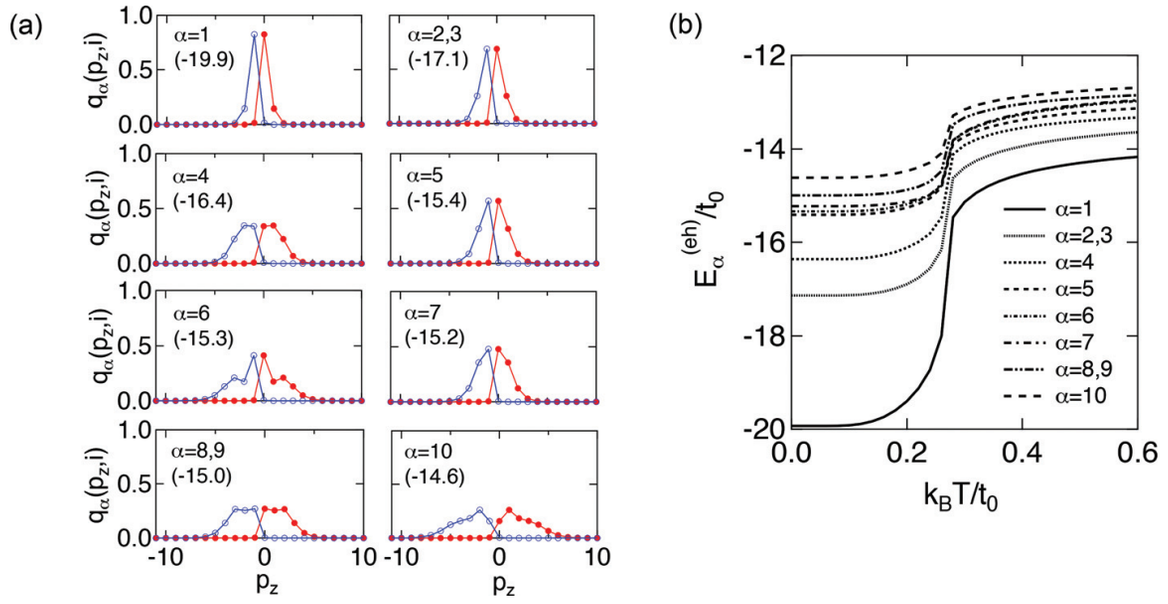

Figure 6. (a) The p_z dependence of electron (filled circle) and hole (open circle) density from the first to 10th eigenstate at $T = 0$. The eigenenergy $E_\alpha^{(eh)}$ is also shown in units of t_0. (b) $E_\alpha^{(eh)}$ as a function of T for $\alpha = 1-10$. The values of U_0/t_0 and w_0/t_0 are set to 10. Figures extracted and edited from Ref. [29].

The critical temperature increases significantly when one of the carriers is localized to only a site near the DA interface, that is, the approximation (II) is employed. This is because such a fixed charge enhances the attractive Coulomb interaction energy through Eqs. (3) and (4) and thus enhances the CTE binding energy significantly. The present result indicates that both the

finite-T and the carrier delocalization effect are important to understand the CTE dissociation at the DA interface.

4. Discussion

4.1. Application to experiments

In this Section, we interpret the recent experimental observations on the CTE dissociation at the DA interfaces. Recently, Gao et al. have studied the charge generation in C_{60}-based organic solar cells through a measurement of the open-circuit voltage in a temperature range from 30 to 290 K. They have found that the number of free carriers created in the solar cells increases with increasing T, where the activation energy for the CTE dissociation is estimated to be 9 and 25 meV in annealed and unannealed systems, respectively [27]. To understand the magnitude of the activation energy, we compute the magnitude of T_c in typical organic solar cells. We set $U_0 = e^2/(4\pi\epsilon d) \simeq 0.5$ eV by using $\epsilon \simeq 3\epsilon_0$ (ϵ_0 is the dielectric constant of vacuum) and the equilibrium molecule-molecule distance $d \simeq 1$ nm of C_{60} crystals. The hopping parameter at the DA interface is set to $t_0 \simeq U_0/10$, by assuming that the single-particle band width is a few hundred meV. The height of the barrier potential is set to $w_0 \simeq U_0$, so that the CTE (not the Frenkel exciton) is formed at T = 0 K. Then, the value of $k_B T_c/t_0 \simeq 0.27$ corresponds to $k_B T_c \simeq 13$ meV. The magnitude of this energy is in agreement with the activation energy reported experimentally [27].

It is noteworthy that the magnitude of the CTE binding energy E_B can be estimated from the EH DOS. Assuming that the continuum states start from $\alpha \simeq 10$ at lower T shown in **Figure 5(a)**, the vth CTE binding energy is $E_B(v) = E^{(eh)}_{\alpha=10} - E^{(eh)}_{\alpha=v}$. For example, $E_B(v = 1) = 5.3\ t_0 \simeq 0.26$ eV, which is an order of magnitude higher than thermal energy at room temperature, but is consistent with experimental observations [15].

4.2. Scenario of the CTE dissociation

The agreement between our theory and experiments implies that the combined effect of the finite-T and carrier delocalization play a major role in the CTE dissociation. Based on our model, we show a possible scenario of the CTE dissociation in **Figure 7**.

1. The exciton is initially created at the donor region by photon absorption.
2. The electron transfer occurs at the DA interface, yielding the CTE formation.
3. The excess energy [32] created by the CTE formation (i.e. the energy difference between the donor LUMO and acceptor LUMO) excites phonons at the interface and disturbs the cold phonon distribution initially at T_0.
4. Through the phonon-phonon and phonon-electron scatterings, the phonon modes will obey the Bose distribution function with temperature T' higher than T_0 after the phonon thermalization time.
5. When T' is larger than T_c, the CTE can dissociate.

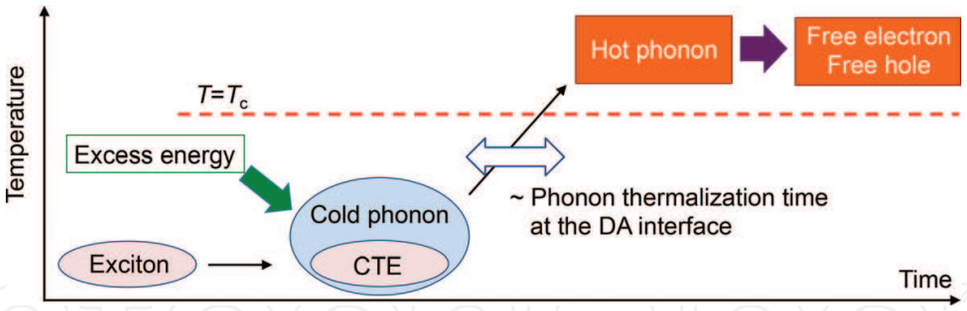

Figure 7. Temperature evolution of the charge carriers and phonons, provided that both the finite T mechanism proposed in the present study and the excess energy mechanism [32] hold. The excess energy created by the CTE formation excites the phonon at the DA interface. The phonon temperature increases with time and becomes over T_c within the phonon thermalization time. Above T_c, the CTE dissociates into the free electron and hole. Figure extracted from Ref. [29].

If this scenario holds, the magnitude of T' gradually increases with time. Then, the CTE energy also increases with time, as expected by the T-dependent $E_\alpha^{(eh)}$ shown in **Figure 6(b)**. This behaviour is quite similar to the experimental observations, where the CTE spontaneously climbs up the Coulomb potential at the pentacene-vacuum interface, by the time-resolved two-photon photoemission spectroscopy [28]. Such a CTE evolution has occurred within 100 fs that may be an order of the period of the optical phonon oscillations. For deeper understanding, it is necessarily to study the time-dependence of the interface phonon temperature T'. This may be studied in the framework of the non-equilibrium theory of phonons [33–35].

4.3. Some remarks

We also emphasize the finite-T effect on the excitonic properties. The exciton is usually described within many-body perturbation theory or time-dependent density-functional theory [36]. Recently, the CTE has been studied in such a first-principles context [37, 38]. The extension to the T-dependent Bethe-Salpeter or time-dependent Kohn-Sham equations and their solutions would give an accurate estimation of the CTE binding energy and predict the localization-delocalization transition or the free-energy anomaly mentioned in the present work.

In the present study, we have assumed that the dielectric constant is homogeneous across the DA interface. Recently, we have studied the effect of the inhomogeneity of the dielectric constant on the charge transfer behaviour within the continuum approach [39]. In such a system, the Coulomb interaction energy between two particles is given by

$$\frac{q_1 q_2}{4\pi\epsilon_0\sqrt{\epsilon(\boldsymbol{r}_1)\epsilon(\boldsymbol{r}_2)}}, \tag{14}$$

where q_i and $\boldsymbol{r}_i$ are the charge and the position of the particle i. $\epsilon(\boldsymbol{r})$ is the local dielectric constant that describes the morphology of the DA interface. By solving the two-particle Schrödinger equation, we have demonstrated that the inhomogeneity of the dielectric constant yields an anisotropy of the charge distribution at the DA interface. Furthermore, we have found that the anisotropic distribution of the hole along the normal to the DA interface is important to yield the electron transfer, or vice versa. More investigation about the relation between the carrier distribution and the interface morphology is desired.

5. Summary

In this chapter, we have derived the T-dependent TB model for a EH pair at the DA interface, which enabled us to study the finite-T as well as the carrier delocalization effect on the CTE dissociation. Our numerical calculations have revealed that there exists the localization-delocalization transition at a critical temperature T_c, above which the CTE dissociates. This is related to the anomaly of the free energy Ω. Below and above T_c, Ω is determined by the internal energy and the entropic energy, respectively. The transition can be observed only when the carrier delocalization treatment is employed. The magnitude of T_c and the CTE binding energy estimated were in agreement with the experimental data. A possible scenario involving the phonon thermalization has been discussed.

So far, the origin of the CTE dissociation has been extensively investigated with consideration of a variety of models. Several effects on the CTE dissociation have been proposed, although the relative impact is not clear. The present study has emphasized the importance of the combined impact of the finite T and the carrier delocalization. Our work would be the first step for understanding the CTE dissociation observed at various DA interface in a unified manner. We hope that the localization-delocalization transition is observed in future experiments.

Acknowledgements

This work was supported by a Grant-in-Aid for Young Scientists B (No. 15K17435) from Japan Society for the Promotion of Science.

Author details

Shota Ono[1]* and Kaoru Ohno[2]

*Address all correspondence to: shota_o@gifu-u.ac.jp

1 Department of Electrical, Electronic and Computer Engineering, Gifu University, Gifu, Japan

2 Department of Physics, Graduate School of Engineering, Yokohama National University, Yokohama, Japan

References

[1] Frenkel J. On the transformation of light into heat in solids. I. Physical Review Journal. 1931;**37**:17

[2] Frenkel J. On the transformation of light into heat in solids. II. Physical Review Journal. 1931;**37**:1276

[3] Wannier G. The structure of electronic excitation levels in insulating crystals. Physical Review Journal. 1937;**52**:191

[4] Elliott RJ. Intensity of optical absorption by excitons. Physical Review Journal. 1957;**108**: 1384

[5] Halls JJM, Cornil J, Dos Santos DA, Silbey R, Hwang D-H, Holmes A B, Brédas JL, Friend RH. Charge- and energy-transfer processes at polymer/polymer interfaces: A joint experimental and theoretical study. Physical Review B. 1999;**60**:5721

[6] Few S, Frost JM, Nelson J. Models of charge pair generation in organic solar cells. Physical Chemistry Chemical Physics. 2015;**17**:2311

[7] Bässler H, Köhler A. "Hot or Cold": How do charge transfer states at the donor-acceptor interface of an organic solar cell dissociate? Physical Chemistry Chemical Physics. 2015;**17**:28451

[8] Hang H, Chen W, Chen S, Qi DC, Gao XY, Wee ATS. Molecular orientation of CuPc thin films on C_{60}/Ag(111). Applied Physics Letters. 2009;**94**:163304

[9] Shih C-F, Hung K-T, Chen H-J, Hsiao C-Y, Huang K-T, Chen S-H. Incorporation of potassium at CuPc/C_{60} interface for photovoltaic application. Applied Physics Letters. 2011;**98**:113307

[10] Lane PA, Cunningham PD, Melinger JS, Kushto GP, Esenturk O, Heilweil EJ. Photoexcitation dynamics in films of C_{60} and Zn phthalocyanine with a layered nanostructure. Physical Review Letters. 2012;**108**:077402

[11] Díaz AS, Burtone L, Riede M, Palomares E. Measurements of efficiency losses in blend and bilayer-type zinc phthalocyanine/C_{60} high-vacuum-processed organic solar cells. Journal of Physical Chemistry C. 2012;**116**:16384

[12] Lane PA, Cunningham PD, Melinger JS, Esenturk O, Heilweil EJ. Hot photocarrier dynamics in organic solar cells. Nature Communications. 2015;**6**:7558

[13] Dowgiallo A-M, Mistry KS, Johnson JC, Blackburn JL. Ultrafast spectroscopic signature of charge transfer between single-walled carbon nanotubes and C_{60}. ACS Nano. 2014;**8**:8573

[14] Ferguson AJ, et al. Trap-limited carrier recombination in single-walled carbon nanotube heterojunction with fullerene accepter layers. Physical Review B. 2015;**91**:245311

[15] Morteani AC, Sreearunothai P, Herz LM, Frend RH, Silva C. Exciton regeneration at polymeric semiconductor heterojunctions. Physical Review Letters. 2004;**92**:247402

[16] Arkhipov VI, Heremans P, Bässler H. Why is exciton dissociation so efficient at the interface between a conjugated polymer and an electron acceptor? Applied Physics Letters. 2003;**82**:4605

[17] Wiemer M, Nenashev AV, Jansson F, Baranovskii SD. On the efficiency of exciton dissociation at the interface between a conjugated polymer and an electron acceptor. Applied Physics Letters. 2011;**99**:013302

[18] Peumans P, Forrest SR. Separation of geminate charge-pairs at donor-acceptor interfaces in disordered solids. Chemical Physics Letters. 2004;**398**:27

[19] Rubel O, Baranovskii SD, Stolz W, Gebhard F. Exact solution for hopping dissociation of geminate electron-hole pairs in a disordered chain. Physical Review Letters. 2008; **100**:196602

[20] Deibel C, Strobel T, Dyakonov V. Origin of the efficient polaron-pair dissociation in polymer-fullerene blends. Physical Review Letters. 2009;**103**:036402

[21] Nenashev AV, Baranovskii SD, Wiemer M, Jansson F, Österbacka R, Dvurechenskii AV, Gebhard F. Theory of exciton dissociation at the interface between a conjugated polymer and an electron acceptor. Physical Review B. 2011;**84**:035210

[22] Raos G, Casalegno M, Idé J. An effective two-orbital quantum chemical model for organic photovoltaic materials. Journal of Chemical Theory and Computation. 2014;**10**:364

[23] Athanasopoulos S, Tscheuschner S, Bässler H, Köhler A. Efficient charge separation of cold charge-transfer states in organic solar cells through incoherent hopping. Journal of Physical Chemistry Letters. 2017;**8**:2093

[24] Schwarz C, Tscheuschner S, Frisch J, Winkler S, Koch N, Bässler H, Köhler A. Role of the effective mass and interfacial dipoles on exciton dissociation in organic donor-acceptor solar cells. Physical Review B. 2013;**87**:155205

[25] Clarke TM, Durrant JR. Charge photogeneration in organic solar cells. Chemical Reviews. 2010;**110**:6736

[26] Gregg B. A. Entropy of charge separation in organic photovoltaic cells: The benefit of higher dimensionality. Journal of Physical Chemistry Letters. 2011;**2**:3013

[27] Gao F, Tress W, Wang J, Inganäs O. Temperature dependence of charge carrier generation in organic photovoltaics. Physical Review Letters. 2015;**114**:128701

[28] Monahan NR, Williams KW, Kumar B, Nuckolls C, Zhu X-Y. Direct observation of entropy-driven electron-hole separation at an organic semiconductor interface. Physical Review Letters. 2015;**114**:247003

[29] Ono S, Ohno K. Combined impact of entropy and carrier delocalization on charge transfer exciton dissociation at the donor-acceptor interface. Physical Review B. 2016;**94**: 075305

[30] Miller A, Abrahams E. Impurity conduction at low concentrations. Physical Review. 1960; **120**:745

[31] Baskoutas S, Terzis AF, Schommers W. Size-dependent exciton energy of narrow band gap colloidal quantum dots in the finite depth square-well effective mass approximation. Journal of Computational and Theoretical Nanoscience. 2006;**3**:269

[32] Jackson NE, Savoie BM, Marks TJ, Chen LX, Ratner MA. The next breakthrough for organic photovoltaics? Journal of Physical Chemistry Letters. 2015;**6**:77

[33] Kabanov VV, Demsar J, Podobnik B, Mihailovic D. Quasiparticle relaxation dynamics in superconductors with different gap structures: Theory and experiments on $YBa_2Cu_3O_{7-\delta}$. Physical Review B. 1999;**59**:1497

[34] Ono S, H Shima, Y Toda. Theory of photoexcited carrier relaxation across the gap of phase-ordered materials. Physical Review B. 2012;**86**:104512

[35] Ono S. Nonequilibrium phonon dynamics beyond the quasiequilibrium approach. To appear in Physical Review B

[36] Onida G, Reining L, Rubio A. Electronic excitations: Density-functional versus many-body Green's-function approaches. Reviews of Modern Physics. 2002;**74**:601

[37] Cudazzo P, Sottile F, Rubio A, Gatti M. Exciton dispersion in molecular solids. Journal of Physics: Condensed Matter. 2015;**27**:113204

[38] Petrone A, Lingerfelt DB, Rega N, Li X. From charge-transfer to a charge-separated state: A perspective from the real-time TDDFT excitonic dynamics. Physical Chemistry Chemical Physics. 2014;**16**:24457

[39] Ono S, Ohno K. Minimal model for charge transfer excitons at the dielectric interface. Physical Review B. 2016;**93**:121301(R)